International Journal of Robotics and Control Systems
Vol. 5, No. 1, 2025, pp. 516-529
ISSN 2775-2658
http://pubs2.ascee.org/index.php/ijrcs

Comparative Analysis of Yolov-8 Segmentation for Gait Performance in Individuals with Lower Limb Disabilities

Resty Wulanningrum [a,b,1], Anik Nur Handayani [a,2,*], Heru Wahyu Herwanto [a,3]

[a] Department of Electrical Engineering and Informatics, Faculty of Engineering, Universitas Negeri Malang, Semarang Street 5, Malang, 65145, East Java, Indonesia
[b] Departement of Informatics Engineering, University of Nusantara PGRI Kediri, Kampus 2, Mojoroto Gang I, No. 6, Mojoroto, Kediri, East Java, Indonesia
[1] resty.wulanningrum.2305349@students.um.ac.id; [2] aniknur.ft@um.ac.id; [3] heru_wh@um.ac.id
* Corresponding Author

ARTICLE INFO

Article history
Received December 05, 2024
Revised January 10, 2025
Accepted January 25, 2025

Keywords
Disabilities;
Gait;
Pattern Recognition;
Yolov8

ABSTRACT

This research aims to develop an example of gait pattern segmentation between normal and disabled individuals. Walking is the movement of moving from one place to another, where individuals with physical limitations on the legs have different walking patterns compared to individuals without physical limitations. This study classifies gait into three categories, namely individuals with assistive devices (crutches), individuals without assistive devices, and normal individuals. The study involved 10 subjects, consisting of 2 individuals with assistive devices, 3 individuals without assistive devices, and 5 normal individuals. The research process was conducted through three main stages, namely: image database creation, data annotation, and model training and segmentation using YOLOv8. YOLOv8-seg is the platform used to segment the data. The test results showed that the YOLOv8L-seg model achieved convergence value at the 23rd epoch with the 4th scenario in recognizing the walking patterns of the three categories. However, research on walking patterns of people with disabilities faces several obstacles, such as the lack of confidence or emotion of the subject during the data collection process, which is conducted at the location of the subject's choice. In addition, YOLOv8-seg showed consistent performance across the five models used, obtaining a maximum mAP50 value of 0.995 for mAP50 box and mAP50 mask.

1. Introduction

Physical disability refers to limitations in bodily functions that affect a person's ability to perform daily activities. It is divided into two main types: lower limb disability [1] and upper limb disability [2]. Lower limb disability includes conditions such as leg amputation [3], paraplegia [4], cerebral palsy [5], [6], and muscular dystrophy [7], which may require assistive devices [8] such as wheelchairs [9] or crutches [10], thus affecting one's gait.

The gait of a normal person has distinctive characteristics [11]. One of them is the upright body position [11]. In this position, the body stands upright and straight [12], maintaining its balance well [13]. This makes the steps taken balanced, with the weight of the body evenly distributed on both feet. In addition, the movements of the arms while walking also look natural. The arms swing freely

with the body movement and help maintain balance. All these factors help in producing an efficient and stable gait.

Abnormal gait includes an upright body position, unbalanced stride, unnatural arm movements, and impairments or injuries [14] that affect gait [15]. G The gait of people with disabilities varies depending on the type and level of disability they experience. They use assistive devices such as canes or wheelchairs to help them walk [16]-[20]. A person with a physical disability in the foot area can also walk without the use of assistive devices. The gait of normal people and people with disabilities can be detected by technology, namely computer vision.

Computer Vision is a subdomain of artificial intelligence that is widely used for image processing [21]-[23]. Cameras and sensors enable computer vision applications. Images and videos are taken, processed, and then analyzed to produce data that is relevant to the application [24]. Computer vision technology in style recognition runs in real-time on normal people [25], [26] by using video recording for detection [27]. Automatic intelligence systems are built by Artificial intelligence (AI), one of which is pattern recognition [28], [29]. Pattern recognition for people's gait [30] aims to identify individuals with different psychological and behavioral characteristics in walking videos [31]. There have been several studies on the gait of normal people, including by Harris [32], Ghersi [33], Taha [34], Alvarez- Aparicio [35], and research on the gait of normal people based on gender [32]. The gait of normal individuals was analyzed using traditional segmentation algorithms, such as edge detection and Convolutional Neural Network (CNN) [33], [34], as well as Otsu threshold-based segmentation [35]. For the segmentation of human objects with background, the Mixture of Gaussian (MOG) method was used [36]. Meanwhile, gait detection of individuals with special conditions was analyzed using YOLO, which generates ankle, knee, and hip kinematic data [37].

The Yolov8 framework developed in 2023 has undergone substantial improvements compared to Yolov7 and Yolov5, resulting in more efficient and accurate performance [38]-[41]. YOLOv8 is the latest object detection model that is more accurate than previous versions by adopting new techniques and optimizations [42], [43]. The YOLO family of object detection [44], [45], and segmentation instances has grown rapidly over the past few years, with each new iteration introducing improvements in accuracy and/or speed [46]. Instance segmentation is a powerful computer vision technique that combines the advantages of object detection and semantic segmentation [47], [48]. The contribution of this research is the application of the Yolov8 algorithm, for instance, segmentation, which is an extension of the segmentation method on the gait patterns of people with disabilities who use assistance, do not use assistance, and are normal.

2. Method

As illustrated in Fig. 1, the detection and segmentation process with Yolov8 consists of three stages: Step 1 involves image creation, Step 2 involves annotation, and Step 3 involves Yolov8.

2.1. Image Base Creation

The first step is Image Base Creation, which is the process of forming the dataset that will be used. This step contains the process of data acquisition from a Readmi Note 5 smartphone device. The video shooting process did not have any special arrangements, considering that the object of research was an individual with a disability. Therefore, extra effort was required to get a suitable video. Individuals with disabilities often have low self-confidence, so when the video is taken, some of them feel embarrassed and even cry. The disabled subjects used in this dataset are from a community of disabled athletes as well as a special school in Kediri, East Java, Indonesia. The video is then carried out through a face-blurring process, which is a stage so that it is not clearly visible on the face, after which video cutting is carried out. Face blurring is one of the ethical efforts to maintain facial confidentiality when using data as a dataset. The participants involved have signed a consent form to be used as research subjects. The video-cutting results are then extracted into 50 images from each video.

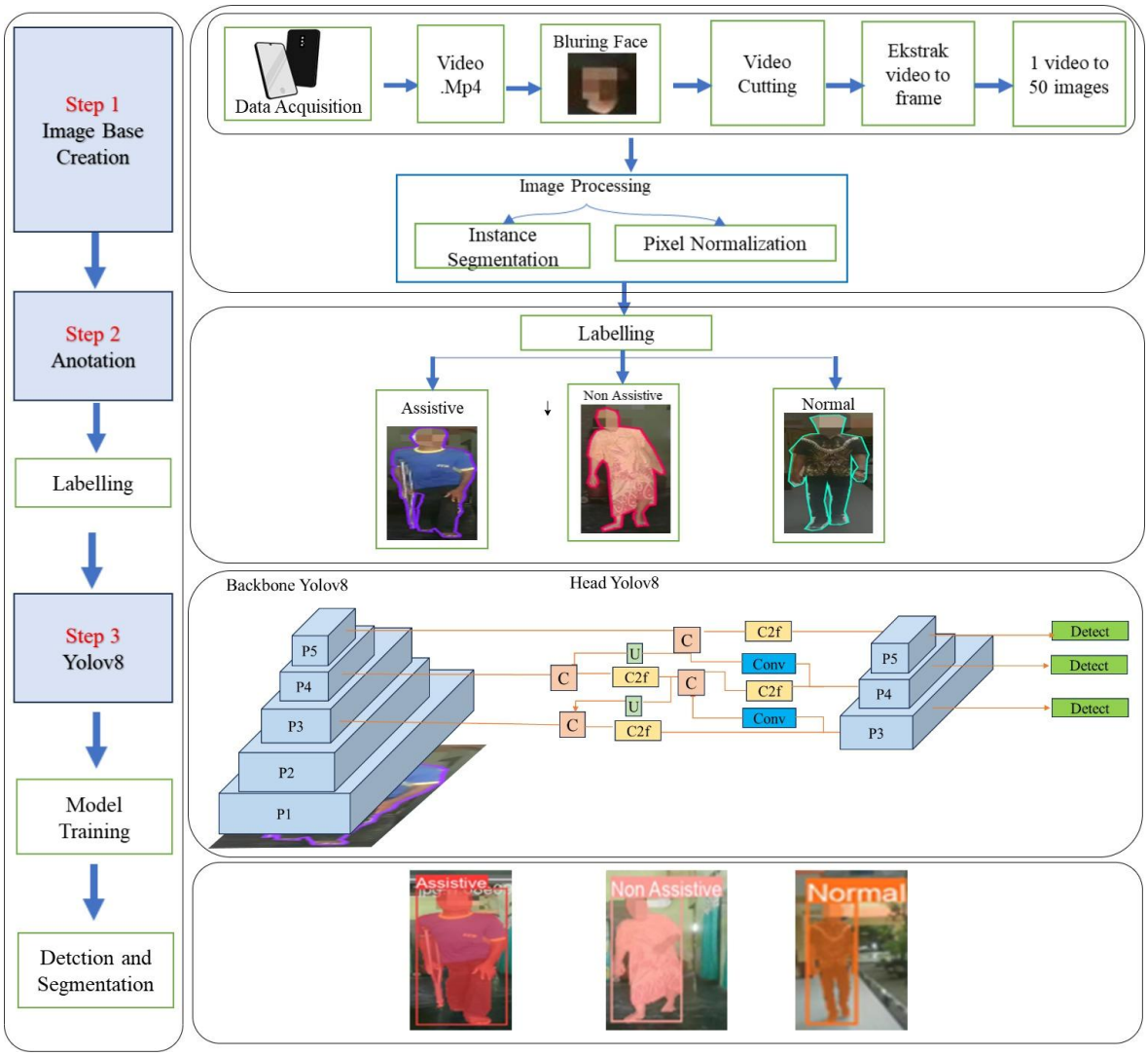

Fig. 1. The Processing of detection and segmentation

Image Base creation is the stage of making the database used in this research. Data Acquisition is the process of taking pictures of the object of research, namely 10 people with disabilities and normal people, consisting of 2 assistive people, three non-assistive people, and five normal people, in the form of videos. The video is blurred so that the face is not visible. The video obtained is then done video cutting, resulting in 13 videos per person, so that there are 130 videos obtained. The next step is to extract video to frame, where 1 video will be extracted into 50 frame images, illustrated in Fig. 2. Next, the stages of instance segmentation and pixel normalization will be carried out.

2.2. Annotation

The images obtained are then subjected to image processing, namely Instance Segmentation and pixel normalization using Roboflow. The second step is annotation, which is labeled into three classes, namely Assistive, Non-Assistive, and Normal. This labeling process has been consulted with a physical disability expert, Dr. Ruruh Andayani Bekti, M. Pd, who is also a trainer of disabled athletes. The third step is the implementation of yolov8 by using the training model. Then, detection and segmentation will be carried out.

Instance segmentation is done using roboflow software and polygon tools to get an instance of person segmentation. The labeling consists of 3 classes, namely assistive, non-assistive, and normal. Assistive means a person with a physical disability in the legs who uses a walker in the form of a cane or crutches. Non-assistive refers to individuals with physical disabilities in the legs who are still able

to walk without the use of assistive devices but have unbalanced and asymmetrical walking patterns like normal people. Meanwhile, it normally refers to individuals who do not have physical disabilities in the legs and are able to walk like most people, with an upright, balanced, and symmetrical walking pattern. The annotation results are illustrated in Fig. 3. The image that has been segmented instances will then be normalized pixels with a size of 640×640 pixels.

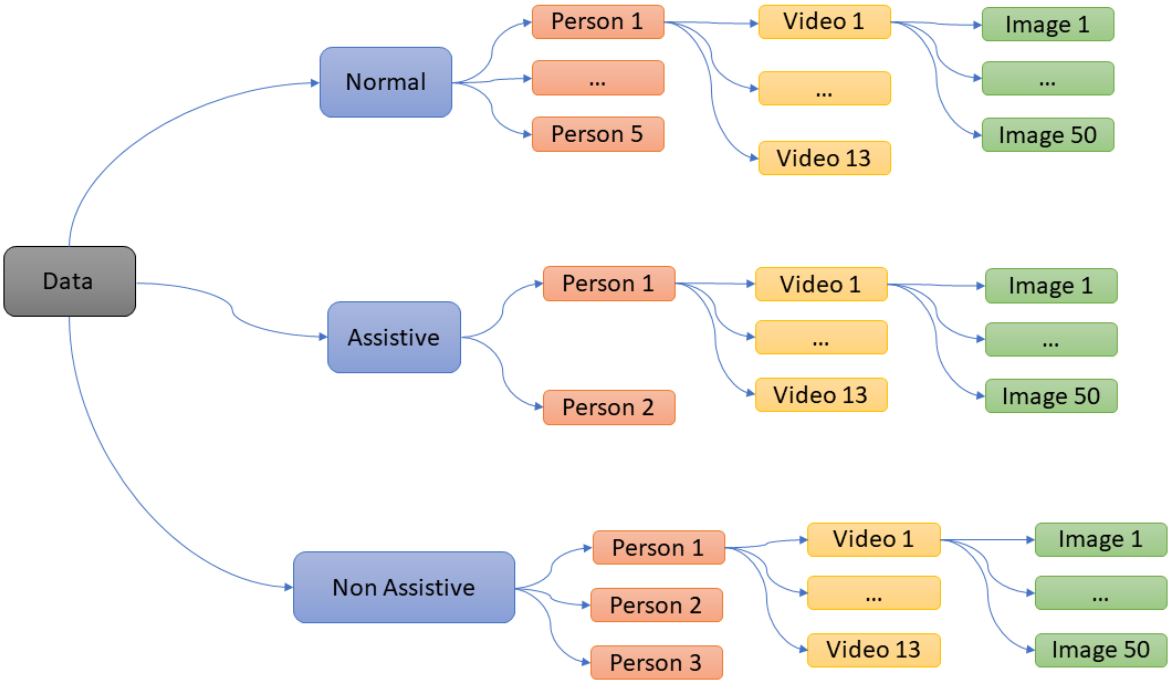

Fig. 2. image structure

Fig. 3. Roboflow annotation result

2.3. Yolov8

The Yolov8 used in this stage is yolov8-seg, which is a variant of the YOLO (You Only Look Once) model specifically designed for the segmentation instance task [49]. The backbone of Yolov8-seg is a convolutional network backbone for extracting features from the input image. The Head part of Yolov8-seg is designed for the segmentation task to predict the segmentation mask for each object detection. It consists of several final convolutions that generate the bounding box, class score, and

segmentation mask for each object. The training data models used in this study are the yolov8n-seg model, the yolov8s-seg model, the yolov8m-seg model, the yolov8l-seg model, and the yolov8x-seg. Table 1 shows the parameters of yolov8- seg that will be used in this study.

Table 1. Yolov8 Model parameters used

Model	Size	mAPbox	mAPmask	Speed	Speed	Params	FLOPs
	(pixels)	50-95	50-95	CPU ONNX (ms)	A100 TensorRT (ms)	(M)	(B)
YOLOv8n-seg	640	36.7	30.5	96.1	1.21	3.4	12.6
YOLOv8s-seg	640	44.6	36.8	155.7	1.47	11.8	42.6
YOLOv8m-seg	640	49.9	40.8	317.0	2.18	27.3	110.2
YOLOv8l-seg	640	52.3	42.6	572.4	2.79	46.0	220.5
YOLOv8x-seg	640	53.4	43.4	712.1	4.02	71.8	344.1

Detection and Segmentation are obtained from the results of custom validation of the training model, which is done by getting the best.pt value for testing validation.

3. Results and Discussion

The training Yolov8-seg model has a 640×640 pixel resolution. The degree of detail necessary for accurate segmentation was balanced with computational efficiency when selecting this image resolution. All experiments were conducted on a Windows 10 Pro PC equipped with an Intel(R) Core (TM) i5-4210U CPU running at 1.70GHz and 2.40GHz, 12.0 GB of RAM, and 64-bit architecture.

3.1. Split Data

The template is designed so that author affiliations are not repeated each time for multiple authors of the same affiliation. Please keep your affiliations as succinct as possible (for example, do not differentiate among departments of the same organization).

Split data in this research test scenario uses 4 test scenarios, namely the first scenario using 70% for training data, 15% for data validation, and 25% for testing data. The second scenario uses 70% training data, 20% validation data, and 10% testing data. Scenario 3 uses 75% for training data, 10% for validation data, and 15% for testing data. Scenario 4 uses 80% for training data, 10% for validation data, and 10% for testing data, as shown in Table 2.

Table 2. Test Scenario

Scenario	Split Data	Training Data	Validation Data	Testing Data
1	701515	70%	15%	25%
2	702010	70%	20%	10%
3	751015	75%	10%	15%
4	801010	80%	10%	10%

3.2. Result of Yolov8 Instance Segmentation

The test results on yolov8-seg have two validation models: label validation and prediction validation. Label validation only mentions assistive, non-assistive, and normal. Meanwhile, the prediction validation provides the results of the confidence score value. For example, the results show assistive 1.0. Will 1.0 indicates the highest confidence score that the detected object really corresponds to the specified class, namely assistive. In other words, the system is very confident that the detected object is assistive (Fig. 4)

Mean Average Precision (mAP) is a metric that measures the overall performance of an object detection [50], [51] model by calculating precision and recall at various prediction thresholds and then averaging them [52], [53]. mAP at IoU 0.5 means that mAP is calculated with an IoU threshold of 0.5 [54].

Steps to Calculate mAP at IoU 0.5

1. Prediction and Ground Truth: For each image in the validation dataset, the model generates a prediction bounding box with a confidence score and class label. The ground truth bounding box is also available for that image.
2. Calculate IoU: For each prediction bounding box, calculate the IoU with the corresponding ground truth bounding box. Equation (1).

$$IoU = \frac{Area\ Of\ Intersection}{Area\ of\ Union} \tag{1}$$

3. Determining True Positive (TP), False Positive (FP), and False Negative (FN):
   a. True Positive (TP): Predicted bounding box that has IoU >= 0.5 with ground truth bounding box and correct prediction class.
   b. False Positive (FP): A bounding box prediction that does not have the corresponding ground truth bounding box (IoU < 0.5) or the wrong prediction class.
   c. False Negative (FN): Ground truth bounding box that does not have a corresponding bounding box prediction (IoU < 0.5).
4. Precision and Recall: Precision: The proportion of TP compared to TP + FP. Equation (2).

$$Precision = \frac{TP}{TP + FP} \tag{2}$$

5. Recall: The proportion of TP compared to TP + FN. Equation (3).

$$Recall = \frac{TP}{TP + FN} \tag{3}$$

6. Precision-Recall Curve:
   a. Create a precision-recall curve by changing the prediction confidence score threshold from 0 to 1.
   b. Calculate the precision and recall at various thresholds.
7. Average Precision (AP): Calculate the area under the precision-recall curve for each object class. This is called Average Precision (AP).
8. Mean Average Precision (mAP): Take the average of the APs for all object classes. This is called mAP. Equation (4).

$$mAP = \frac{1}{2}\sum_{i=1}^{N} AP_i \tag{4}$$

Where N is the number of object classes.

The mAP50 (Box) value measures how well the model detects and localizes objects with a bounding box [55], while mAP50 (Mask) measures how well the model detects and describes detailed object shapes with a mask [56]. In the tests conducted, the value of mAP50(B) is the same as the value of mAP50(M) shown in Fig. 5.

3.3. Discussion

Mean Average Precision at IoU 0.5, often abbreviated as mAP50 in the 4 test scenarios conducted, the minimum and maximum values of each scenario and model test are sought. The results of the max mAP value and four scenarios and model tests show the same maximum value of mAP 50, which is at a value of 0.995, illustrated in Table 3. Overfitting indicates that the model has learned

too specifically on the training data, thus failing to generalize to new data. This can happen if the training data has characteristics that are too uniform or if the dataset used has not gone through an augmentation process to increase variation. Meanwhile, high model performance in training or testing datasets does not necessarily guarantee good performance in the real world, as real-world data tends to be more diverse. These variations include changes in lighting, object orientation, and complex situations that may not be fully represented in the training or testing data.

Fig. 4. Label validation and prediction results

Table 3. mAP 50 value results from 4 test scenarios

Scenario	Yolov8n-seg		Yolov8s-seg		Yolov8m-seg		Yolov8l-seg		Yolov8x-seg	
	Min	Max	Min	Max	Min	Max	Min	Max	Min	Max
1	0.06659	0.995	0.7825	0.995	0.94461	0.995	0.97217	0.995	0.94445	0.995
2	0.0653	0.995	0.7789	0.995	0.94461	0.995	0.96708	0.995	0.94753	0.995
3	0.30328	0.995	0.82592	0.995	0.97177	0.995	0.94917	0.995	0.98257	0.995
4	0.30328	0.995	0.35803	0.995	0.74313	0.995	0.93895	0.995	0.91992	0.995

In the tests conducted on four scenarios in Table 4, a minimum mAP50 value of 0.3028 and a maximum mAP50 value of 0.995 were obtained. This larger range may indicate instability or variability in model performance. Several factors, such as uneven data distribution, suboptimal training methods, or model sensitivity to certain parameters may cause such instability. This is dependent on the quality of the training process's dataset. Accurate and consistent annotations help the model learn effectively. Additionally, the diversity of the dataset, which includes a variety of objects, backgrounds, lighting conditions, and viewing angles, ensures that the model can generalize well. Since the dataset includes images of people with disabilities taken in real-world settings where the subjects chose the location, the data is varied with many backgrounds, lighting conditions, and suboptimal viewpoints. The min-max value is obtained from the difference between the highest mAP50 value and the lowest mAP50 value during training in each scenario. For example, in scenario 1 for the Yolov8l-Seg model, the highest value was 0.995, while the lowest value was 0.9721. Thus, the min-max value distance is calculated as follows:

$$Max - Min = 0.995 - 0.9721 = 0.02283$$

Table 4. Range of min- max distance at mAP50

Scenario	Yolov8n-seg	Yolov8s-seg	Yolov8m-seg	Yolov8l-seg	Yolov8x-seg
1	0.92841	0.2125	0.05039	0.02283	0.05055
2	0.9297	0.2161	0.05039	0.02792	0.04747
3	0.69172	0.16908	0.02323	0.04583	0.01243
4	0.69172	0.63697	0.25187	0.05605	0.07508

The selection of the test model and the best test scenario in this study can be seen in the convergence value of the test at what epoch value? Tests on convergence and epoch are in Table 5.

Table 5. Convergence epoch on Yolov8-seg modelConvergence on training data is seen in scenario each model has an epoch convergence value of 99 and 98 on yolov8n-seg in scenarios 1 and 2. Scenario 3 at epoch 14 has experienced convergence, but in scenario 4, it rises again, converging at epoch 37. On yolov8s-seg, it looks to have the same convergence at epoch 57 in scenarios 1 and 2. While convergence at epoch 40 in scenario 3 and convergence at epoch 22 in scenario 4. The increase in convergence of each scenario has a stable value, but because the value of the min-max range is still too far apart, then yolov8s-seg is not the best in this research.

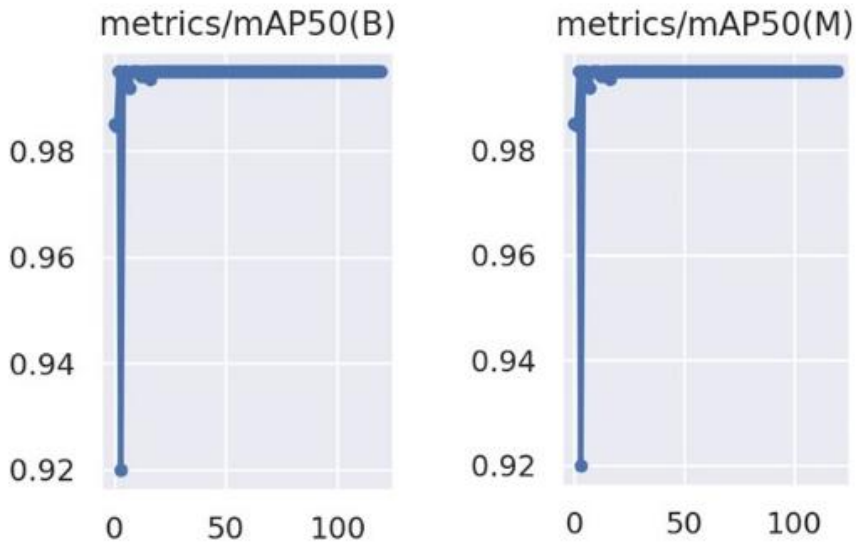

Fig. 5. Map 50 (B) and mAP 50 (M) results

Yolov8m-seg also has the same convergence value in scenarios 1 and 1 at epoch 84. Yolov8l-seg has convergence at epoch 18 in scenario 3 and experienced an increase in convergence in scenario 4, namely at epoch 42. Yolov8l-seg has convergence at epoch 65 in scenarios 1 and 2. At epoch 24, it experienced convergence in scenario three and convergence of epoch 23 in scenario 4. In this yolov8l-seg, which has the lowest and most stable minimum and maximum range values seen from the mAP50 value. In yolov8x-seg has a convergence value at epoch 21 in scenarios 1 and 2. Convergence at epoch 52 in scenario three and convergence at epoch 17 in scenario 3. When viewed from the results of scenarios related to the value of convergence, scenarios 1 and 2 have training data as much as 70% of the total data. It can be concluded that the higher the training value, the lower the epoch convergence value that occurs in the case of datasets for assistive, non-assistive, and normal recognition.

Fig. 6 depicts the tests in scenario 4. This indicates that the mAP50 value reached epochs 14–22, declined at epoch 23, and then started to converge again at epoch 24. These changes were caused by box_loss and seg_loss. Box_loss increased by 0.0149, resulting in a decrease in results that prevented convergence. Relationship between box_loss and seg_loss shown in Table 5.

Data Explanation Table:

1. Box_loss of Training vs Validation:

a. The box_loss in training gradually decreases from 0.71753 (Epoch 14) to about 0.64518 (Epoch 24). This indicates that the model is getting better at predicting the bounding box during training.

b. The validation box_loss also shows a decrease (e.g., from 0.50613 to 0.41733), which reflects better generalization of the model to the validation data.

2. Training vs. Validation Seg_loss:

a. The training seg_loss shows more variable values (e.g., 10.702 at Epoch 14 and a drastic decrease to 0.98325 at Epoch 25). This decrease could indicate that the model is starting to handle segmentation better despite the initial large values.

b. In the validation data, seg_loss tends to be stable, with small fluctuations from 0.74806 to around 0.71952. This relatively constant value could indicate the stability of the model's performance on the segmentation task.

This study compares 5 yolov8-seg models for the gait of disabled and normal people. The model evaluation uses the mAP50 value with box and mask values. The research that has been done found a model that shows that the mAP50 box and mask values are the same. When added objects and datasets are added, it will affect the results of the evaluation of the mAP50 value on the box and mask. The use of changing data scenarios will affect the distance or range of mAP50 values. The values of box_loss and seg_loss also affect the mAP50 value so that it can cause underfitting or overfitting.

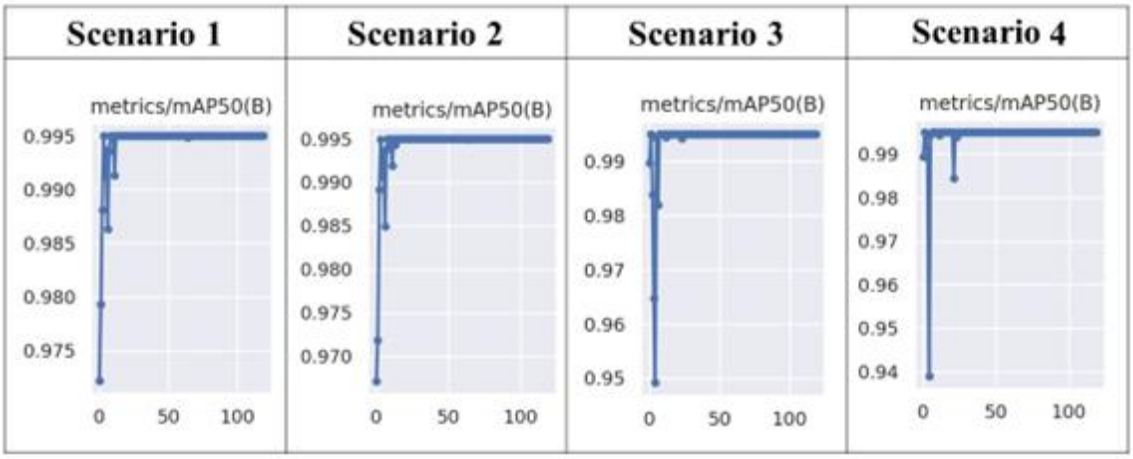

Fig. 6. mAP50 value of yolov8l- seg

Table 5. Relationship between box_loss and seg_loss

Epoch	Train		Epoch	Valid	
	Box_loss	Seg_loss		Box_loss	Seg_loss
14	0.71753	10.702.00	14	0.50613	0.74806
15	0.70947	11.023.00	15	0.44159	0.72531
16	0.69649	10.372.00	16	0.48738	0.77173
17	0.70705	10.586.00	17	0.46925	0.74413
18	0.69493	10.493.00	18	0.45774	0.73859
19	0.68981	11.206.00	19	0.41764	0.74214
20	0.6661	10.333.00	20	0.45293	0.74208
21	0.66499	1.048.00	21	0.39075	0.74796
22	0.66648	0.97948	22	0.44437	0.70847
23	0.68657	1.007.00	23	0.45165	0.72343
24	0.64518	10.594.00	24	0.41733	0.72808
25	0.65621	0.98325	25	0.44149	0.71952

This study has several important implications that can serve as a reference for further development. Firstly, the consistency of the mAP50 box and mask values suggests that the model can

be uniformly used for bounding box and mask segmentation evaluation on similar data. Secondly, increasing the number of objects or varying the dataset can affect the performance of the model, so testing on various datasets is necessary to ensure the generalizability of the model. Thirdly, varying data scenarios can also affect the mAP50 value, so it is important to test the model under various conditions to determine performance tolerances. In addition, the box_loss and seg_loss values are directly related to mAP50, indicating that optimization of these two parameters during training is necessary to avoid underfitting or overfitting. Evaluation using mAP50 also provides an initial indication of model quality, but further research is still needed to understand the effects of additional factors, such as dataset complexity or usage scenarios. Finally, the model has the potential to be further developed to effectively detect and analyze the gait of people with disabilities and normal people in various conditions, such as in rehabilitation or health monitoring applications. All these implications can serve as guidelines for further research or real-world implementation of the model.

4. Conclusion

This study proposes the YOLOv8-seg framework to detect and classify three gait classes in people with disabilities, namely assistive, non-assistive, and normal disabilities, by comparing five variants of the YOLOv8-seg model. The evaluation results showed consistent performance across the five models, with a maximum mAP50 of 0.995 for both box and mask metrics, where the YOLOv8l-seg model and the 4th test scenario gave the best results with convergence at the 23rd epoch. While these findings are promising, further research is needed to ensure the robustness of the model against more diverse and complex datasets, such as variations in resolution, illumination, and the presence of anomalies or mislabeling, to improve generalizability. In addition, testing in real-world scenarios and in-depth analysis of the box_loss and seg_loss parameters are needed to avoid overfitting and improve performance. Further validation and development, such as integration in portable devices for rehabilitation or video-based real-time applications, are promising potential areas to optimize the implementation of this model to support comprehensive gait analysis.

Author Contribution: Resty Wulanningrum: Conceptualization, Methodology, Software, Writing Anik Nur Handayani: Data curation, Writing- Original draft preparation. Heru Wahyu Herwanto: Visualization, Validation, Reviewing and Editing

Funding: This research received no external funding

Acknowledgment: This research did not receive any specific grant from funding agencies in the public, commercial, or not-for-profit sectors

Conflicts of Interest: The authors declare no conflict of interest.

References

[1] S. Okano *et al*., "ATP1A3 potentially causes hereditary spastic paraplegia: A case report of a patient presenting with lower limb spasticity and intellectual disability," *Brain and Development Case Reports*, vol. 2, no. 2, p. 100016, 2024, https://doi.org/10.1016/j.bdcasr.2024.100016.

[2] A. S. E. Alreni, H. R. Abdo Aboalmaty, W. De Hertogh, J. Meirte, D. Harrop, and S. M. McLean, "Measuring upper limb disability for patients with neck pain: Evaluation of the feasibility of the single arm military press (SAMP) test," *Musculoskeletal Science and Practice*, vol. 50, p. 102254, 2020, https://doi.org/10.1016/j.msksp.2020.102254.

[3] L. Shelmerdine and G. Stansby, "Lower limb amputation and rehabilitation," *Surgery*, vol. 40, no. 7, pp. 445–449, 2022, https://doi.org/10.1016/j.mpsur.2022.05.015.

[4] D. G. Calame *et al*., "Cation leak through the ATP1A3 pump causes spasticity and intellectual disability," *Brain*, vol. 146, no. 8, pp. 3162-3171, 2023, https://doi.org/10.1093/brain/awad124.

[5] I. F. Pérez, T. B. Villagra, J. Jiménez-Balado, J. J. Redondo, and B. B. Recasens, "Risk factors and outcome of epilepsy in adults with cerebral palsy or intellectual disability," *Epilepsy & Behavior*, vol. 147, p. 109450, 2023, https://doi.org/10.1016/j.yebeh.2023.109450.

[6] A. S. Faradyza *et al*., "Real Time Gesture Detection Using Kinect in Rehabilitation Therapy for Children with Disability," *2021 7th International Conference on Electrical, Electronics and Information Engineering (ICEEIE)*, pp. 452-456, 2021, https://doi.org/10.1109/ICEEIE52663.2021.9616817.

[7] A. C. Klimchak, L. Sedita, K. L. Gooch, and D. C. Malone, "EE291 Ethical Implications of Quality-Adjusted Life Year Assessments for Patients with Disabilities: A Duchenne Muscular Dystrophy Case Study," *Value in Health*, vol. 26, no. 6, p. S112, 2023, https://doi.org/10.1016/j.jval.2023.03.592.

[8] J. J. Kim, J. Lee, J. Shin, and M. He, "How are high-tech assistive devices valued in an aging society? Exploring the use and non-use values of equipment that aid limb disability," *Technology in Society*, vol. 70, p. 102013, 2022, https://doi.org/10.1016/j.techsoc.2022.102013.

[9] M. Kayama, G. Yan, A. Adams, and R. J. Miles, "'The wheelchair really is just a piece of athletic equipment to play the sport of basketball': The experience of college athletes with disabilities navigating social inclusion and exclusion," *Children and Youth Services Review*, vol. 155, p. 107251, 2023, https://doi.org/10.1016/j.childyouth.2023.107251.

[10] F. Rasouli and K. B. Reed, "Walking assistance using crutches: A state of the art review," *Journal of Biomechanics*, vol. 98, p. 109489, 2020, https://doi.org/10.1016/j.jbiomech.2019.109489.

[11] M. Bendt, E. B. Forslund, G. Hagman, C. Hultling, Å. Seiger, and E. Franzén, "Gait and dynamic balance in adults with spina bifida," *Gait Posture*, vol. 96, pp. 343–350, 2022, https://doi.org/10.1016/j.gaitpost.2022.06.016.

[12] C. Mazzà, M. Zok, and U. Della Croce, "Sequencing sit-to-stand and upright posture for mobility limitation assessment: determination of the timing of the task phases from force platform data," *Gait Posture*, vol. 21, no. 4, pp. 425–431, 2005, https://doi.org/10.1016/j.gaitpost.2004.05.006.

[13] A. A. da Silva Costa *et al*., "Corticomuscular and intermuscular coherence as a function of age and walking balance difficulty," *Neurobiology of Aging*, vol. 141, pp. 85–101, 2024, https://doi.org/10.1016/j.neurobiolaging.2024.05.004.

[14] I. A. E. Zaeni, D. Lestari, A. N. Handayani, and M. K. Osman, "Development of Stride Detection System for Helping Stroke Walking Training," *Journal of Electronics, Electromedical Engineering, and Medical Informatics*, vol. 5, no. 3, pp. 159–167, 2023, https://doi.org/10.35882/jeemi.v5i3.306.

[15] A. Alfayyadh *et al*., "Unbalanced Medial-to-Lateral Knee Muscle Co-Contractions are Associated with Medial Tibiofemoral Underloading during Gait Three Months after Anterior Cruciate Ligament Reconstruction," *Journal of Biomechanics*, vol. 163, p. 111925, 2024, https://doi.org/10.1016/j.jbiomech.2024.111925.

[16] J. Nie, M. Jiang, A. Botta, and Y. Takeda, "An adaptive gait event detection method based on stance point for walking assistive devices," *Sensors and Actuators A: Physical*, vol. 364, p. 114842, 2023, https://doi.org/10.1016/j.sna.2023.114842.

[17] D. Matsuura, Y. Chounan, M. Omata, Y. Sugahara, and Y. Takeda, "Chapter 2 - Gait analysis and regeneration by means of principal component analysis and its application to kinematic design of wearable walking assist device for hemiplegics," *Design and Operation of Human Locomotion Systems*, pp. 33–49, 2020, https://doi.org/10.1016/B978-0-12-815659-9.00002-0.

[18] W.-Y. Huang, S.-H. Tuan, M.-H. Li, and P.-T. Hsu, "Efficacy of a novel walking assist device with auxiliary laser illuminator in stroke Patients~ a randomized control trial," *Journal of the Formosan Medical Association*, vol. 121, no. 3, pp. 592–603, 2022, https://doi.org/10.1016/j.jfma.2021.06.019.

[19] B. Feodoroff and V. Blümer, "Unilateral non-electric assistive walking device helps neurological and orthopedic patients to improve gait patterns," *Gait Posture*, vol. 92, pp. 294–301, 2022, https://doi.org/10.1016/j.gaitpost.2021.11.016.

[20] K. Nakagawa *et al*., "Short-term effect of a close-fitting type of walking assistive device on spinal cord reciprocal inhibition," *Journal of Clinical Neuroscience*, vol. 77, pp. 142–147, 2020, https://doi.org/10.1016/j.jocn.2020.04.121.

[21] E.-S. Kim, Y. Oh, and G. W. Yun, "Sociotechnical challenges to the technological accuracy of computer vision: The new materialism perspective," *Technology in Society*, vol. 75, p. 102388, 2023, https://doi.org/10.1016/j.techsoc.2023.102388.

[22] M. Ciranni, V. Murino, F. Odone, and V. P. Pastore, "Computer vision and deep learning meet plankton: Milestones and future directions," *Image and Vision Computing*, vol. 143, p. 104934, 2024, https://doi.org/10.1016/j.imavis.2024.104934.

[23] A. P. Wibawa, W. A. Yudha Pratama, A. N. Handayani, and A. Ghosh, "Convolutional Neural Network (CNN) to determine the character of wayang kulit," *International Journal of Visual and Performing Arts*, vol. 3, no. 1, pp. 1–8, 2021, https://doi.org/10.31763/viperarts.v3i1.373.

[24] N. Ottakath, A. Al-Ali, S. Al-Maadeed, O. Elharrouss, and A. Mohamed, "Enhanced computer vision applications with blockchain: A review of applications and opportunities," *Journal of King Saud University - Computer and Information Sciences*, vol. 35, no. 10, p. 101801, 2023, https://doi.org/10.1016/j.jksuci.2023.101801.

[25] A. Parashar, A. Parashar, A. F. Abate, R. S. Shekhawat, and I. Rida, "Real-time gait biometrics for surveillance applications: A review," *Image and Vision Computing*, vol. 138, p. 104784, 2023, https://doi.org/10.1016/j.imavis.2023.104784.

[26] U. Gawande, K. Hajari, and Y. Golhar, "Real-Time Deep Learning Approach for Pedestrian Detection and Suspicious Activity Recognition," *Procedia Computer Science*, vol. 218, pp. 2438–2447, 2023, https://doi.org/10.1016/j.procs.2023.01.219.

[27] M. H. Khan, M. S. Farid, and M. Grzegorzek, "Vision-based approaches towards person identification using gait," *Computer Science Review*, vol. 42, p. 100432, 2021, https://doi.org/10.1016/j.cosrev.2021.100432.

[28] A. Larasati, A. M. Hajji, and A. N. Handayani, "Identification of Learning Characteristics Pattern of Engineering Students using Clustering Techniques," *Proceedings of the 2nd International Conference on Learning Innovation ICLI - Volume 1*, pp. 274–278, 2019, https://doi.org/10.5220/0008411002740278.

[29] M. C. Bagaskoro, F. Prasojo, A. N. Handayani, E. Hitipeuw, A. P. Wibawa, and Y. W. Liang, "Hand image reading approach method to Indonesian Language Signing System (SIBI) using neural network and multi layer perseptron," *Science in Information Technology Letters*, vol. 4, no. 2, pp. 97–108, 2023, https://doi.org/10.31763/sitech.v4i2.1362.

[30] G. Li, L. Guo, R. Zhang, J. Qian, and S. Gao, "TransGait: Multimodal-based gait recognition with set transformer," *Applied Intelligence*, vol. 53, no. 2, pp. 1535–1547, 2023, https://doi.org/10.1007/s10489-022-03543-y.

[31] Y. Liu, C. Wang, H. Li, and Y. Zhou, "Gait recognition of camouflaged people based on UAV infrared imaging," *Infrared Physics & Technology*, vol. 138, p. 105262, 2024, https://doi.org/10.1016/j.infrared.2024.105262.

[32] R. A. Asmara *et al*., "Comparative Study of Gait Gender Identification using Gait Energy Image (GEI) and Gait Information Image (GII)," *MATEC Web of Conferences,* vol. 197, p. 15006, 2018, https://doi.org/10.1051/matecconf/201819715006.

[33] J. Luo, H. Wu, L. Lei, H. Wang, and T. Yang, "GCA-Net: Gait contour automatic segmentation model for video gait recognition," *Multimedia Tools and Applications*, vol. 81, no. 24, pp. 34295–34307, 2022, https://doi.org/10.1007/s11042-021-11248-6.

[34] M. M. Islam, S. Nooruddin, F. Karray, and G. Muhammad, "Human activity recognition using tools of convolutional neural networks: A state of the art review, data sets, challenges, and future prospects," *Computers in Biology and Medicine*, vol. 149, p. 106060, 2022, https://doi.org/10.1016/j.compbiomed.2022.106060.

[35] D. Balta, I. Cocchi, F. Molinari, U. Della Croce, and A. Cereatti, "A comparative study of three segmentation algorithms for 2-dimensional markerless gait analysis," *Gait & Posture*, vol. 74, p. 4, 2019, https://doi.org/10.1016/j.gaitpost.2019.07.447.

[36] S. Sivolobov, "Human gait feature extraction method," *Procedia Computer Science*, vol. 193, pp. 220–227, 2021, https://doi.org/10.1016/j.procs.2021.10.022.

[37] M. S. Rana, "Leveraging Markerless Computer Vision for Comprehensive Walking Automated Gait Analysis in Rehabilitation," *Master's Thesis*, 2024, https://www.theseus.fi/bitstream/handle/10024/860826/Rana_Md_Shohel.pdf?sequence=2&isAllowed=y.

[38] R. Sapkota, D. Ahmed, and M. Karkee, "Comparing YOLOv8 and Mask R-CNN for instance segmentation in complex orchard environments," *Artificial Intelligence in Agriculture*, vol. 13, pp. 84-99, 2024, https://doi.org/10.1016/j.aiia.2024.07.001.

[39] J. Terven and D. Cordova-Esparza, "A Comprehensive Review of YOLO Architectures in Computer Vision: From YOLOv1 to YOLOv8 and YOLO-NAS," *Machine Learning and Knowledge Extraction*, vol. 5, no. 4, pp. 1680-1716, 2023, https://doi.org/10.3390/make5040083.

[40] A. Aboah, B. Wang, U. Bagci and Y. Adu-Gyamfi, "Real-time Multi-Class Helmet Violation Detection Using Few-Shot Data Sampling Technique and YOLOv8," *2023 IEEE/CVF Conference on Computer Vision and Pattern Recognition Workshops (CVPRW)*, pp. 5350-5358, 2023, https://doi.org/10.1109/CVPRW59228.2023.00564.

[41] Y. Zhang, Y. Lu, W. Zhu, X. Wei, and Z. Wei, "Traffic sign detection based on multi-scale feature extraction and cascade feature fusion," *The Journal of Supercomputing*, vol. 79, no. 2, pp. 2137–2152, 2023, https://doi.org/10.1007/s11227-022-04670-6.

[42] C. Zhang, X. Chen, P. Liu, B. He, W. Li, and T. Song, "Automated detection and segmentation of tunnel defects and objects using YOLOv8-CM," *Tunnelling and Underground Space Technology*, vol. 150, p. 105857, 2024, https://doi.org/10.1016/j.tust.2024.105857.

[43] A. Mourato, J. Faria, and R. Ventura, "Automatic sunspot detection through semantic and instance segmentation approaches," *Engineering Applications of Artificial Intelligence*, vol. 129, p. 107636, 2024, https://doi.org/10.1016/j.engappai.2023.107636.

[44] R. A. Asmara, B. Syahputro, D. Supriyanto and A. N. Handayani, "Prediction of Traffic Density Using YOLO Object Detection and Implemented in Raspberry Pi 3b + and Intel NCS 2," *2020 4th International Conference on Vocational Education and Training (ICOVET)*, pp. 391-395, 2020, https://doi.org/10.1109/ICOVET50258.2020.9230145.

[45] R. A. Asmara *et al*., "YOLO-based object detection performance evaluation for automatic target aimbot in first-person shooter games," *Bulletin of Electrical Engineering and Informatics*, vol. 13, no. 4, pp. 2456–2470, 2024, https://doi.org/10.11591/eei.v13i4.6895.

[46] Y. Choi, B. Bae, T. Hee Han and J. Ahn, "Application of Mask R-CNN and YOLOv8 Algorithms for Concrete Crack Detection," *IEEE Access*, vol. 12, pp. 165314-165321, 2024, https://doi.org/10.1109/ACCESS.2024.3469951.

[47] A. M. Hafiz and G. M. Bhat, "A survey on instance segmentation: state of the art," *International Journal of Multimedia Information Retrieval*, vol. 9, no. 3, pp. 171–189, 2020, https://doi.org/10.1007/s13735-020-00195-x.

[48] F. Barrientos-Espillco, M. J. Gómez-Silva, E. Besada-Portas, and G. Pajares, "Integration of object detection and semantic segmentation based on convolutional neural networks for navigation and monitoring of cyanobacterial blooms in lentic water scenes," *Applied Soft Computing*, vol. 163, p. 111849, 2024, https://doi.org/10.1016/j.asoc.2024.111849.

[49] A. Tharatipyakul, T. Srikaewsiew, and S. Pongnumkul, "Deep learning-based human body pose estimation in providing feedback for physical movement: A review," *Heliyon*, vol. 10, no. 17, p. e36589, 2024, https://doi.org/10.1016/j.heliyon.2024.e36589.

[50] C. Zhang *et al*., "Evaluation of the YOLO models for discrimination of the alfalfa pollinating bee species," *Journal of Asia-Pacific Entomology*, vol. 27, no. 1, p. 102195, 2024, https://doi.org/10.1016/j.aspen.2023.102195.

[51] Q. Li, W. Ma, H. Li, X. Zhang, R. Zhang, and W. Zhou, "Cotton-YOLO: Improved YOLOV7 for rapid detection of foreign fibers in seed cotton," *Computers and Electronics in Agriculture*, vol. 219, p. 108752, 2024, https://doi.org/10.1016/j.compag.2024.108752.

[52] Y. Peng *et al*., "A dynamic individual method for yak heifer live body weight estimation using the YOLOv8 network and body parameter detection algorithm," *Journal of Dairy Science*, vol. 107, no. 8, pp. 6178–6191, 2024, https://doi.org/10.3168/jds.2023-24065.

[53] C. Xiong, T. Zayed, and E. M. Abdelkader, "A novel YOLOv8-GAM-Wise-IoU model for automated detection of bridge surface cracks," *Construction and Building Materials*, vol. 414, p. 135025, 2024, https://doi.org/10.1016/j.conbuildmat.2024.135025.

[54] Q. Wang *et al*., "Enhanced recognition of insulator defects on power transmission lines via proposal-based detection model with integrated improvement methods," *Engineering Applications of Artificial Intelligence*, vol. 136, p. 109078, 2024, https://doi.org/10.1016/j.engappai.2024.109078.

[55] S. A. Mostafa *et al*., "A YOLO-based deep learning model for Real-Time face mask detection via drone surveillance in public spaces," *Information Sciences*, vol. 676, p. 120865, 2024, https://doi.org/10.1016/j.ins.2024.120865.

[56] J. Chen, C. Ji, J. Zhang, Q. Feng, Y. Li, and B. Ma, "A method for multi-target segmentation of bud-stage apple trees based on improved YOLOv8," *Computers and Electronics in Agriculture*, vol. 220, p. 108876, 2024, https://doi.org/10.1016/j.compag.2024.108876.